COURSE-KEEPING SIMULATIONS OF A SHIP IN CONFINED WATERWAYS BASED ON INTEGRATED CFD METHOD AND CONTROL ALGORITHM

Zi-Qiang Zheng, School of Ocean and Civil Engineering, Shanghai Jiao Tong University, China

Yu He, School of Ocean and Civil Engineering, Shanghai Jiao Tong University, China

Lu Zou, School of Ocean and Civil Engineering, Shanghai Jiao Tong University, China

Zao-Jian Zou, School of Ocean and Civil Engineering, Shanghai Jiao Tong University, China

COURSE-KEEPING SIMULATIONS OF A SHIP IN CONFINED WATERWAYS BASED ON INTEGRATED CFD METHOD AND CONTROL ALGORITHM

ZI-QIANG ZHENG, SCHOOL OF OCEAN AND CIVIL ENGINEERING, SHANGHAI JIAO TONG UNIVERSITY, CHINA
YU HE, SCHOOL OF OCEAN AND CIVIL ENGINEERING, SHANGHAI JIAO TONG UNIVERSITY, CHINA
LU ZOU*, SCHOOL OF OCEAN AND CIVIL ENGINEERING, SHANGHAI JIAO TONG UNIVERSITY, CHINA
ZAO-JIAN ZOU, SCHOOL OF OCEAN AND CIVIL ENGINEERING, SHANGHAI JIAO TONG UNIVERSITY, CHINA

SUMMARY

The course-keeping problem of a ship model in confined waterways is investigated by numerical simulations coupled with a control algorithm in the present study. The URANS method is applied to simulate viscous flows around the ship, and the overset mesh technique combined with the PD algorithm is adopted to realize the rudder action during course keeping. To improve simulation efficiency, the body-force propeller is applied and a virtual bank method is developed to simplify the modeling of bank effects. The results of free-running simulations indicate that the bank-induced yaw moment is the dominant factor causing ship-bank collisions in confined waterways. Applying the controller in simulations, the ship successfully achieves course keeping with either initial off-centerline deviation or heading angle. Furthermore, the simulated flow field indicates that the ship deviates a small distance from the waterway centerline during course keeping to overcome the additional sway force and yaw moment induced by propeller-rudder interaction.

NOMENCLATURE

B	Breadth (m)
d	Draft (m)
D	Propeller diameter (m)
Fr	Froude number based on ship length (-)
Fr_h	Froude number based on water depth (-)
g	Acceleration of gravity (m/s^2)
h	Water depth (m)
K_d	Derivative gain (-)
K_p	Proportional gain (-)
L_{pp}	Length between perpendiculars (m)
N	Yaw moment (Nm)
N_{bank}	Bank yaw moment (Nm)
N_{hydro}	Hydrodynamic yaw moment (Nm)
r	Yaw rate (rad/s)
u	Surge velocity (m/s)
U_0	Nominal speed (m/s)
v	Sway velocity (m/s)
W	Channel width (m)
X	Surge force (N)
Y	Sway force (N)
Y_{bank}	Bank sway force (N)
Y_{hydro}	Hydrodynamic sway force (N)
β	Drift angle (°)
δ	Rudder angle (°)
η	Off-centerline deviation (m)
η_0	Initial off-centerline deviation (m)
λ	Scale ratio (-)
ρ	Fluid density (kg/m^3)
ψ	Heading angle (°)
ψ_0	Initial heading angle (°)

1 INTRODUCTION

Ship maneuverability in confined waterways has garnered continuous attention. The increase in ship size causes reductions in the under keel clearance (UKC) and the navigable waterway width, leading to more significant shallow-water and bank effects. Under the influences of shallow-water and bank effects, a ship navigating in confined waterways experiences additional sway force and yaw moment (Delefortrie, 2024a). These additional force and moment tend to push the ship off its intended course, increasing the collision risks with the banks (Yuan, 2019). This issue becomes particularly pronounced with the rapid development of large-scale ships. Consequently, ship steering and control become significantly more difficult. A reliable autopilot control strategy for keeping ship course in confined waterways could effectively improve navigation efficiency and safety. Therefore, investigations on ship maneuverability and control strategies are of critical importance.

So far, significant progress has been made in studying ship hydrodynamic performances in confined waterways with the perspective of the quasi-steady assumption (the ship is fixed and water flows to the ship) or captive state (the ship moves along a specified trajectory), by applying model tests (Norrbin, 1975; Vantorre et al., 2002; Vantorre et al., 2003; Lataire et al., 2009; Van Zwijnsvoorde et al., 2022; Delefortrie, 2024a; Delefortrie, 2024b), potential flow theory (Yao and Zou, 2010; Zhou et al., 2012; Yuan, 2016; Ren et al., 2020; Degrieck et al., 2021; Xu et al., 2024; Terziev et al., 2024), and viscous flow methods (Zou, 2012; Zou and Larsson, 2013; Van Hoydonck et al., 2019; Liu et al., 2021; Lee, 2023; Terziev et al., 2024). These studies focused on evaluating the hydrodynamic performance of ships in captive motions, without considering motions in multiple freedoms or dynamic rudder action, which were inadequate for practical navigation applications. Consequently, there is a pressing need for studies focusing on ship maneuvering and control under such conditions. The most common approach is computational simulations based on mathematical models (i.e., ship motion equations). By solving the ship motion equations, the motion parameters and ship trajectory at specified rudder angle and propeller speed can be directly calculated. The key and premise of this approach are to establish an appropriate mathematical model.

Captive model tests are the most reliable approach to identify the hydrodynamic parameters in mathematical model. For instance, Fujino (1968, 1970), Sano et al. (2012, 2014), and Yasukawa (2019) carried out captive model tests for different ships and waterway configurations. The mathematical models were established based on the measured forces and moments in the model tests, and then the corresponding maneuverability was investigated. However, such model tests require specialized facilities, such as shallow-water towing tanks or facilities with “false” bottoms and banks, significantly increasing their complexity and cost. Furthermore, these tests fail to provide detailed flow information, limiting their ability to analyze the underlying mechanisms of shallow-water and bank effects on ship maneuverability and control performance. Although the numerical methods can provide detailed flow mechanisms, the mathematical modeling based on numerically determined hydrodynamic parameters from prescribed captive motions is still confronted with challenges in practical applications.

In contrast, direct simulations of maneuvering motions based on the Computational Fluid Dynamics (CFD) method tend to be a viable alternative for this problem. CFD-based approaches address many limitations of model tests, eliminating the need for extensive physical experiments (so-called free-running tests) and enabling the interpretation of detailed flow field results. The CFD simulations provide deeper insights into hydrodynamic interactions and offer practical guidance for ship navigation in confined waterways. Up to now, direct simulations have been successfully applied to ship maneuvering and control in open water, shallow waters, and waves (Carrica et al., 2016; Wang et al., 2017; Kim et al., 2022; Kim et al., 2023), demonstrating their satisfactory abilities. However, their applications to confined-water problems remain challenging due to the complexities of simulating both the fully coupled hull-propeller-rudder system and the surrounding viscous flows within these restricted environments.

Based on the above background, this paper employs CFD-based simulations coupled with control actions to address the course-keeping problem of a ship in confined waterways. The objective is to improve the capability of CFD simulations for providing in-depth analyses of hydrodynamic mechanism for a moving ship under bank effects in confined waterways, and to offer control guidance coupled with the simulations for keeping ship course in such environments. To this end, the unsteady Reynolds Averaged Navier-Stokes (URANS) method is utilized to simulate the viscous flows around the ship, and the overset mesh technique is adopted to realize the dynamic rudder deflection during the control action. In addition, a virtual bank treatment is developed to significantly simplify the inherent numerical complexity and to improve computing efficiency while considering the bank effects on the ship motion. Two typical types of scenarios in confined waterways are investigated: one is the ship navigating with an initial off-centerline deviation and the other is the ship navigating with an initial heading angle, representing common scenarios in practical applications where external disturbances or improper operations may influence the ship course.

2 STUDY OBJECT AND SIMULATION CONDITIONS

2.1 SHIP MODEL

The benchmark ship model: KRISO Container Ship (KCS) is selected as the target ship for this study. The main particulars of the hull, propeller, and rudder are presented in Table 1, and their geometries are illustrated in Figure 1. It should be noted that the rudder stock is also ignored for simplification.

Table 1. Main particulars of hull, propeller and rudder

	Parameter	Symbol	Unit	Value
Hull	Scale ratio	λ	-	1:52.667
	Length between perpendiculars	L_{pp}	m	4.367
	Breadth	B	m	0.611
	Draft	d	m	0.205
Propeller	Diameter	D	m	0.15
	Blade number	-	-	5
	Hub ratio	-	-	0.227
	Rotation direction	-	-	right
Rudder	Rudder area	-	m^2	0.0415
	Lateral area	-	m^2	0.0196

Figure 1. KCS model geometry

2.2 COORDINATE SYSTEMS

Two right-handed coordinate systems are adopted to describe the ship location and motion parameters, as shown in Figure 2. The first one is the earth-fixed coordinate system o_0-$x_0y_0z_0$, where the o_0-x_0y_0 plane is placed on the undisturbed water surface, the x_0-axis is along the waterway centerline, and the z_0-axis points vertically downward. The other one is the ship-fixed coordinate system *o-xyz*. Its origin is set at the midship, the *x*-axis and the *y*-axis point toward the bow and the starboard, respectively. The position and direction of the target ship are described by the midship coordinates (x_0, y_0) in o_0-$x_0y_0z_0$ and the heading angle ψ (angle between x_0 and *x* axes). The positive heading angle ψ and rudder angle δ are illustrated in Figure 2. In addition, force components: *X* (surge force), *Y* (sway force), *N* (yaw moment) and velocity components: *u* (surge velocity), *v* (sway velocity), *r* (yaw rate) are defined in *o-xyz*. The off-centerline deviation η is the distance between the midship and the centerline (η=y_0). The ship location is also presented in nondimensional form:

$$x_0' = x_0 / L_{pp},\ \eta' = y_0 / L_{pp} \tag{1}$$

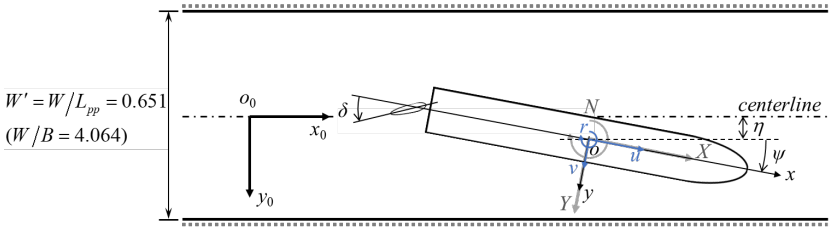

Figure 2. Definition of coordinate systems

2.3 SIMULATION CONDITIONS

The course-keeping performance of the target ship in the waterway is numerically investigated in this paper. The waterway cross-section is rectangular with a water depth h = 0.41m (h/d = 2.0) and a width W = 2.483m ($W' = W/L_{pp}$ = 0.651, W/B = 4.064). The blockage factor is defined as the ratio of the midship-sectional area below the water surface to the cross-sectional area of the waterway. The value is 0.122 in the present study, corresponding to a moderate confined-water condition. Two types of scenarios in confined waterways are investigated: one is the ship navigating with an initial off-centerline deviation $\eta_0' = \pm 0.127$ (Case1), and the other is the ship navigating with an initial heading angle $\psi_0 = \pm 2°$ (Case2), as shown in Table 2 and Figure 3. In the simulations, the target ship starts to move in the straight-ahead motion and is free to surge, sway and yaw (three degrees of freedom). The propeller revolution rate is fixed at 330 RPM according to the self-propulsion point in model tests (Delefortrie et al., 2012), corresponding to the nominal ship speed U_0 = 0.62 m/s. The Froude

number based on ship length $Fr = U_0 / \sqrt{gL_{pp}}$ is 0.095, while the Froude number based on water depth $Fr_h = U_0 / \sqrt{gh}$ is 0.309.

Table 2. Simulation conditions

	Case No.	η_0'	ψ_0 (°)	h/d	W'
Initial off-centerline deviation	Case1-1	0.127	0	2.0	0.651
	Case1-2	−0.127	0		
Initial heading angle	Case2-1	0	2		
	Case2-2	0	−2		

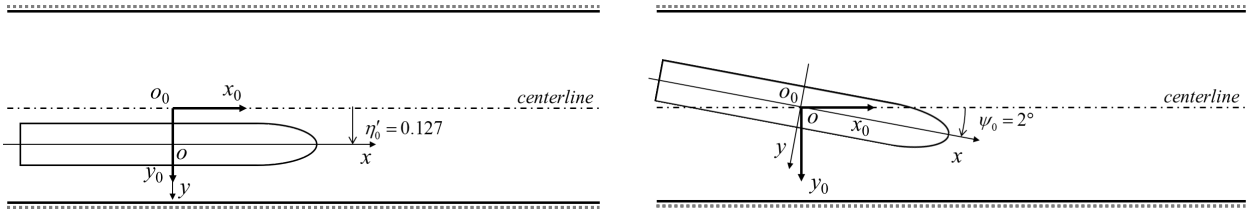

(a) Case1-1 ($\eta_0' = 0.127$) **(b) Case2-1 ($\psi_0 = 2°$)**

Figure 3. Diagram of simulation conditions

3 NUMERICAL METHODS AND SETTINGS

3.1 GOVERNING EQUATIONS

The viscous flow around the ship is assumed to be incompressible. The time-averaged continuity equation and unsteady RANS equations are adopted as the governing equations:

$$\begin{cases} \dfrac{\partial \overline{u}_i}{\partial x_i} = 0 \\ \dfrac{\partial \overline{u}_i}{\partial t} + \dfrac{\partial}{\partial x_j}\left(\overline{u}_i \overline{u}_j\right) = -\dfrac{1}{\rho}\dfrac{\partial \overline{p}}{\partial x_i} + \dfrac{1}{\rho}\dfrac{\partial}{\partial x_j}\left(\overline{\sigma}_{ji} - \rho\overline{u_i' u_j'}\right) + f_i \end{cases} \tag{2}$$

where $\overline{u}_{i(j)}$, $\overline{p}$ and $\overline{\sigma}_{ji}$ denote the time-averaged velocity, pressure and stress tensor components (i, j=1, 2, 3); f_i is the body force, which is regarded as a constant term; $-\rho\overline{u_i' u_j'}$ represents the Reynolds stresses. In this study, the SST k-ω turbulence model (Menter, 1993) is applied to close the governing equations. Simulations are conducted by the STAR-CCM+ software.

3.2 VIRTUAL BANK METHOD

The strategy for free-running simulations of ship maneuvering motion under rudder actions in confined waterways differs significantly from those in open waters, as illustrated in Figure 4. Due to relative motions between the ship and the bank, the narrow waterway with physical bank walls (no-slip walls) in close proximity to the ship must be accurately modeled to mimic the real-world scenario of a ship navigating a confined waterway. It is flexible to apply the dynamic overset mesh technique to handle the complex relative motions between ship and bank. Furthermore, appropriate mesh refinements along the ship trajectory are essential to ensure interpolation accuracy between the background and overset domains (Zheng et al., 2023). These constraints significantly increase computational complexity and cost. To address these challenges, the present study adopts a simplification that effectively reflects the confined-waterway effects while reducing computational costs.

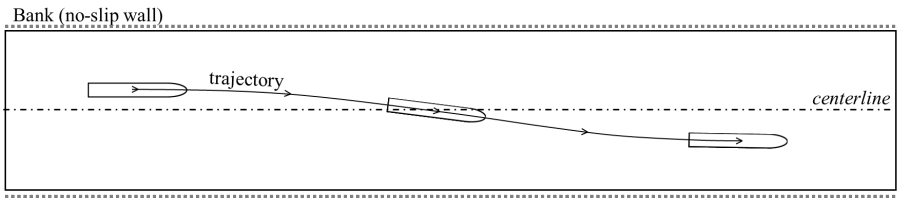

Figure 4. Numerical simulation strategy for confined waterways

A virtual bank method is developed in the present study to simplify the physical wall modeling while still accounting for the bank effects, as shown in Figure 5. In this method, the ship motion in open water with limited water depth is directly simulated, while the additional forces and moments caused by the side bank are directly imposed on the ship in the simulation by formulating the bank effects based on hydrodynamic parameters, without modeling the real bank walls in the simulations. The formulas describe the functional correlation between the bank-induced sway force, yaw moment, and relevant hydrodynamic parameters, which may affect the ship course-keeping motions. This treatment effectively addresses the inherent limitations in traditional numerical simulation strategies for confined-water problems. According to the mathematical model of a ship navigating in confined waterways (Sano et al., 2014), the sway force Y_{bank} and yaw moment N_{bank} induced by the bank can be expressed by the following formulas:

$$\begin{cases} Y_{bank} = 0.5\rho L_{pp} d U_0^2 \left(Y'_{\eta}\eta' + Y'_{\beta\beta\eta}\beta^2\eta' + Y'_{\beta\eta\eta}\beta\eta'^2 + Y'_{\eta\eta\eta}\eta'^3 + Y'_{\eta\eta\delta}\eta'^2\delta \right) \\ N_{bank} = 0.5\rho L_{pp}^2 d U_0^2 \left(N'_{\eta}\eta' + N'_{\beta\beta\eta}\beta^2\eta' + N'_{\beta\eta\eta}\beta\eta'^2 + N'_{\eta\eta\eta}\eta'^3 + N'_{\eta\eta\delta}\eta'^2\delta \right) \end{cases} \tag{3}$$

where ρ denotes fluid density, and β is the drift angle. In this paper, the hydrodynamic derivatives in Eq. (3) are obtained by regressing the Froude number Fr using the experimental results (Sano et al., 2014). As a result, the resultant sway force Y and yaw moment N acting on the ship can be expressed as follows:

$$\begin{cases} Y = Y_{hydro} + Y_{bank} \\ N = N_{hydro} + N_{bank} \end{cases} \tag{4}$$

where Y_{hydro} and N_{hydro} denote the hydrodynamic sway force and yaw moment respectively in shallow- and open-water simulations without the impacts by the side bank.

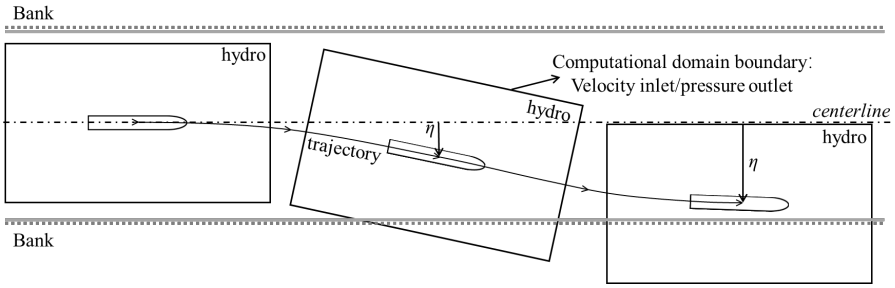

Figure 5. Schematic diagram of virtual bank method

3.3 CONTROL ALGORITHM

The course keeping in simulations is achieved by maintaining the heading angle ψ close to zero under rudder actions. The rudder is controlled by a Proportional-Derivative (PD) algorithm with the following control mechanism:

$$\delta = -K_p\psi - K_d r \tag{5}$$

where K_p and K_d represent proportional and derivative gains, respectively. Both gains are determined through a systematic tuning process, guided by the objective of achieving stable and satisfactory control performance for the course-keeping purpose in the confined waterway. During the tuning process, the proportional gain K_p is first adjusted to achieve a reasonable response speed of the ship, then the derivative gain K_d is applied to improve stability and reduce oscillations in the ship motion. The final set of gains is selected based on a balance between response speed and robustness under the studied conditions. Based on the tuning process, both are set to 10.

3.4 BODY-FORCE PROPELLER MODEL

Since modeling the actual propeller rotation in numerical simulations requires extremely small time steps and highly refined mesh discretization (Deng et al., 2022), it becomes computationally expensive, especially for course-keeping simulations involving rudder actions. Therefore, in the present study, the propeller is modeled using the body-force method (Sørensen, 2022), as its performance and accuracy for simulating ship maneuvering motions have been validated by Aram and Mucha (2023) and Mucha et al. (2023). This approach does not model the geometry and rotation of the propeller blades. Instead, the propeller effects are represented by introducing body forces into the momentum conservation equations. The propeller thrust and torque are derived from open-water propeller performance curves, which provide the thrust coefficient (K_T) and torque coefficient (K_Q) as functions of the advance ratio (J). By distributing these forces over the region where the propeller operates, the body-force method efficiently captures the propeller impact on the flow field while significantly reducing computational costs.

3.5 COMPUTATIONAL DOMAIN

The computational domain is illustrated in Figure 6. The overset mesh technique is utilized to simulate the relative motion between the hull and rudder. Consequently, there are two domains in the simulations: a background domain and an overset domain for the rudder. The distances between the boundaries of the background domain and the ship are sufficient to ensure that these boundaries do not disturb the flow around the ship. In the simulations, the ship is moving forward at a self-propulsion state by the body-force propeller model. The boundary conditions are set as: bottom plane, hull and rudder surfaces are specified as the no-slip walls, while the other boundaries of the background domain are set as the pressure outlet. The overset domain closely envelops the rudder and rotates with it during the simulation, as shown in Figure 6(b).

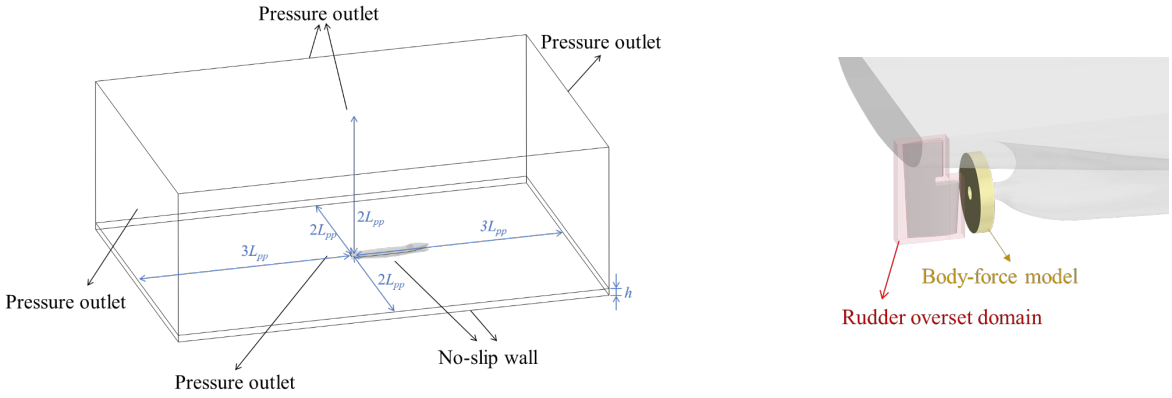

(a) Background domain **(b) Rudder overset domain**

Figure 6. Computational domain

3.6 MESH DISCRETIZATION

The trimmed mesh and prism layer mesh are applied to discretize the computational domain, and an illustration of the mesh distribution is shown in Figure 7. The prism layer mesh is used to generate orthogonal prismatic cells next to the hull and rudder surfaces. For these complex simulations involving rudder rotation and propeller propulsion, mesh refinements for these critical regions are employed to more precisely capture the details in the flow field, as shown in Figures 7(b)–(d). As a result, a total of 2.75 million mesh cells (2.63 million for the background domain and 0.13 million for the overset domain) are generated for the simulation. Given the more frequent rudder deflections during the initial navigation phase in confined waterways, the time step is set to 0.01 s for the first 100 s simulation and adjusted to 0.02 s thereafter.

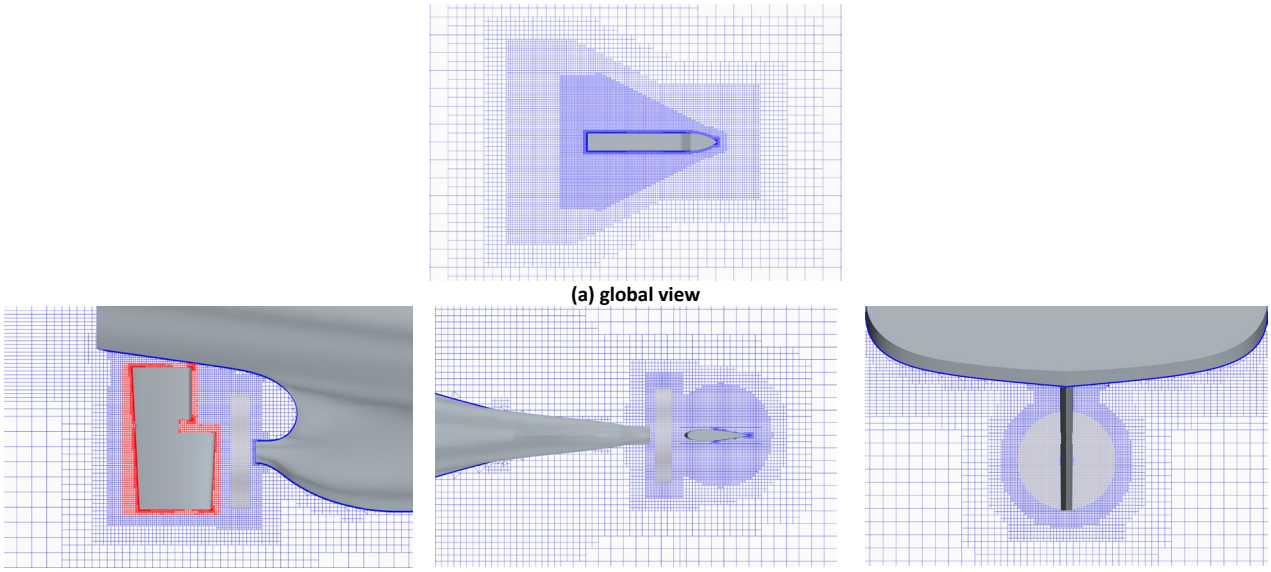

(a) global view

(b) local side view **(c) local bottom view** **(d) local stern view**

Figure 7. Mesh distributions

4 SIMULATION RESULTS

4.1 UNCONTROLLED CONDITIONS

Two scenarios with a total of four cases under both uncontrolled and controlled conditions are simulated for comparison. First, in order to demonstrate the feasibility of the applied virtual bank method and highlight the significance of the controller for ship navigation in confined waterways, Figure 8 shows the ship trajectory under the uncontrolled condition until it collides with the bank. The figure includes a set of simplified ship profiles indicating its position and orientation at several snapshots in time (red lines). The results indicate that even minimal initial disturbances (an initial off-centerline deviation or an initial heading angle) will lead to ship collisions with the waterway bank. Furthermore, the simulations reveal that all collisions occur in less than 40 s, implying that a ship navigating in confined waterways under the uncontrolled condition will be apt to collide with the bank walls. The results confirm that the virtual bank method effectively models the bank effects that cause the ship to deviate from its intended course. It is also observed that the time to collision with the starboard bank is significantly shorter than that with the port bank with the same amount of initial disturbance or deviation. It may be attributed to the right-handed propeller, which generates the wake flow interacting with the rudder. Overall, these findings emphasize the necessity of applying a ship controller for maintaining course-keeping in confined waterways.

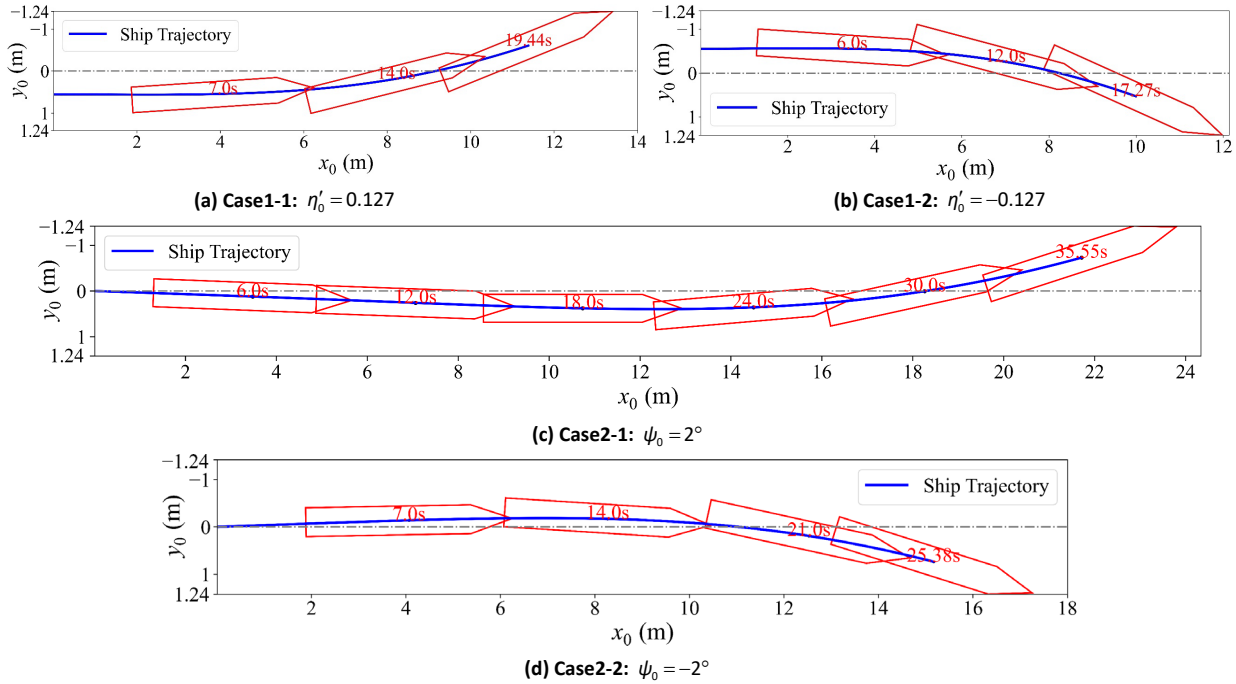

(a) Case1-1: $\eta_0' = 0.127$

(b) Case1-2: $\eta_0' = -0.127$

(c) Case2-1: $\psi_0 = 2°$

(d) Case2-2: $\psi_0 = -2°$

Figure 8. Ship trajectory under the uncontrolled condition

To further analyze the mechanism of bank effects, taking Case1-2 and Case2-2 as examples, the nondimensional off-centerline deviation η, heading angle ψ, sway force Y, yaw moment N, and velocity components u, v, r are shown in Figure 9. For Case1-2, although the ship is initially closer to the portside bank, the consistent impact of the bank effects causes the bow to be attracted to the bank on the other side. From the perspective of forces and moments acting on the ship, the resultant sway force Y repels the ship toward the starboard bank throughout most of the motion in the waterway. Meanwhile, the variation of the resultant yaw moment N is more complex, exhibiting a pattern of bow attraction, repulsion, and then attraction to the starboard bank. Regarding the sway force, positive values indicate a motion tendency of the ship toward the bank wall on the starboard side, while negative values signify a tendency toward the wall on the port side. The initial off-centerline deviation generates a bank-induced sway force Y_{bank}. During the navigation process, Y_{bank} consistently attracts the ship toward the closer bank wall. However, since the magnitude of Y_{hydro} is larger than that of Y_{bank}, it is demonstrated that Y_{hydro} attracting the ship to the starboard side is more dominant.

For the yaw moment, positive values indicate that the ship turns the bow toward the wall on the starboard side, while negative values mean that the ship turns the bow toward the wall on the port side. The direction of N_{bank} is opposite to that of N_{hydro} nearly all the time, but N_{bank} with a greater magnitude has a more pronounced effect than N_{hydro} during the motion. The variation of N_{bank} is more complex: firstly, it is imposed on the ship from the beginning of the motion and consistently exists until the ship passes through the centerline ($0 < x_0' < 1.887$). At this phase, N_{bank} tends to repel the bow away from the closer bank on the port side, hence the yaw rate r and the heading angle ψ continuously increase. After the ship crosses

the centerline ($x_0' > 1.887$), N_{bank} turns positive and then negative, inducing a bow repulsion-attraction trend. Consequently, the yaw rate r first increases and then decreases, while the heading angle ψ continues to increase due to the consistently positive r. Along with the large heading angle, the ship forward motion ultimately leads to a collision with the bank.

For Case2-2 with an initial heading angle $\psi_0 = -2°$, as shown in Figure 9(b), it can be similarly observed that the Y_{hydro} and N_{bank} with greater magnitudes are more dominant during the navigation process. The former attracts the ship toward the starboard bank consistently, while the latter firstly tends to turn the bow toward the starboard bank before the ship crosses the centerline ($0 < x_0' < 2.528$), and then changes its direction after crossing the centerline ($x_0' > 2.528$). Consequently, the yaw rate r firstly increases and then decreases correspondingly. Due to the constantly positive value of r, the heading angle ψ is consistently increasing throughout this process. With the continuous propulsion, the ship ultimately collides with the starboard bank.

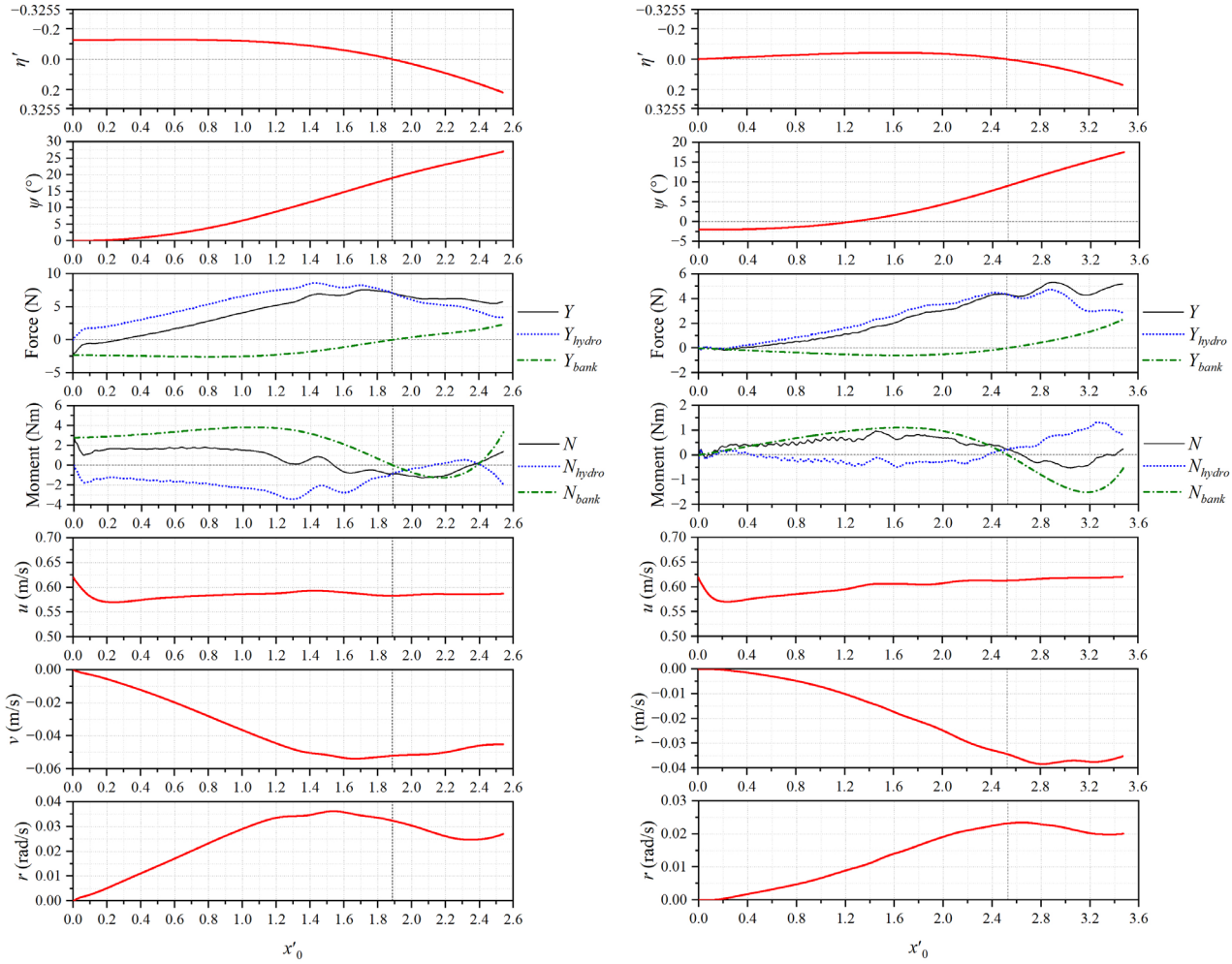

(a) Case1-2: $\eta_0' = -0.127$ **(b) Case2-2:** $\psi_0 = -2°$

Figure 9. Simulation results under the uncontrolled condition

4.2 CONTROLLED CONDITIONS

The results in Section 4.1 highlight the significance of the rudder controller for course keeping when the ship moves in confined waterways. In this section, the simulations for the same scenarios but under the controlled condition are conducted to illustrate the effectiveness of the controller formulated by Eq. (5). The actual trajectories for the four cases are presented in Figure 10, with y_0 magnified 10 times for clarity. It can be observed that after approximately 160 s the trajectories stabilize into quasi-linear paths, indicating successful course-keeping performances. This confirms the effectiveness of the applied control algorithm for course-keeping. In particular, it is interesting to note that in all cases the controlled ship course deviates by approximately 0.2 m from the centerline, since the zero heading angle is selected as the control goal, not the zero deviation from the waterway centerline.

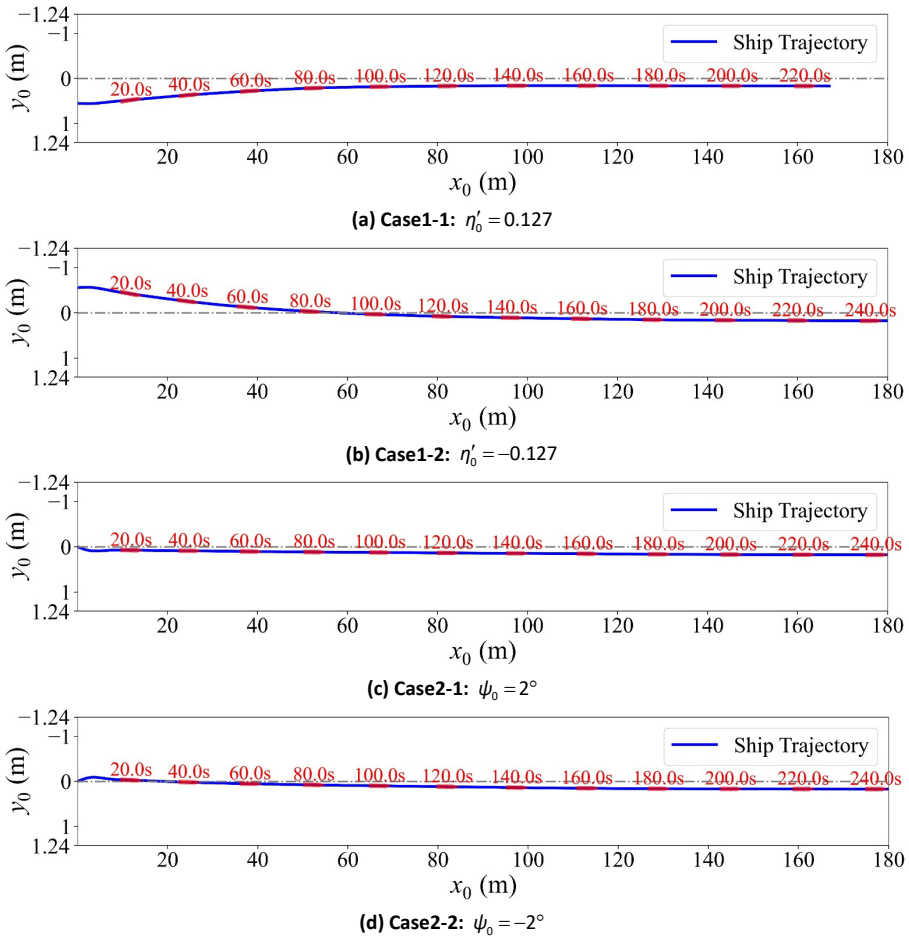

(a) Case1-1: $\eta_0' = 0.127$

(b) Case1-2: $\eta_0' = -0.127$

(c) Case2-1: $\psi_0 = 2°$

(d) Case2-2: $\psi_0 = -2°$

Figure 10. Ship trajectory under the controlled condition

Similar to Section 4.1, the nondimensional location, heading angle ψ, rudder angle δ, sway force Y, yaw moment N, and velocity components u, v, r for Case1-2 and Case2-2 are shown in Figure 11. The time histories of the heading angle ψ demonstrate that the applied controller effectively guides the heading angle to approach zero and maintain this target course in both cases. From the time histories of the rudder angle δ, significant rudder deflection is observed during the initial phases of both cases to control the heading angle. It is noteworthy that after the ship motion tends to be stable with zero heading angle, the ship experiences two pairs of stable sway forces (Y_{hydro} and Y_{bank}) and yaw moments (N_{hydro} and N_{bank}), which have nearly equal magnitudes but opposite directions. As a result, the resultant sway force Y and yaw moment N are close to zero. The stable bank sway force Y_{bank} and yaw moment N_{bank} are attributed to the constant off-centerline deviation $\eta' \approx 0.046$, while the inherent hydrodynamic sway force Y_{hydro} and moment N_{hydro} on the ship in straight-ahead motions are likely induced by the asymmetrical flow field generated by the propeller rotation, and propeller-induced flows are interacted with the rudder.

To confirm it, Figure 12 exhibits the streamlines around the rudder and the pressure distributions on the surface during the course-keeping process. It illustrates that the rotating propeller generates a circumferential flow downstream passing the rudder. This asymmetric flow between the port and starboard sides of the rudder leads to an imbalance in the pressure distributions, producing a lateral force on the rudder. Consequently, the ship experiences additional sway force Y_{hydro} and yaw moment N_{hydro} in straight-ahead motions even without a rudder angle. Finally, the ship is forced to slightly deviate from the centerline to allow the bank force Y_{bank} and moment N_{bank} to counterbalance the additional hydrodynamic sway force Y_{hydro} and yaw moment N_{hydro}.

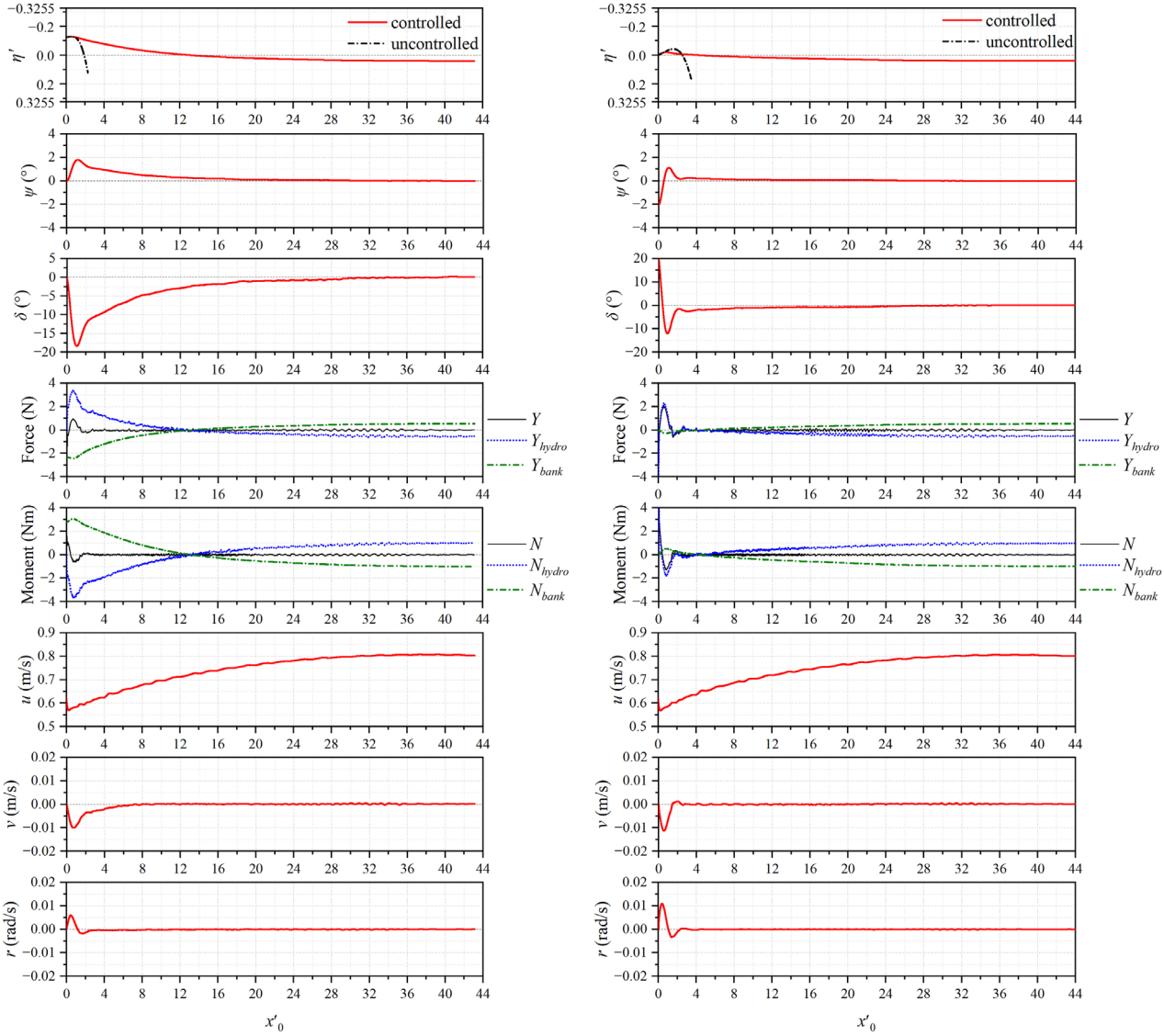

(a) Case1-2: $\eta_0' = -0.127$ **(b) Case2-2:** $\psi_0 = -2°$

Figure 11. Simulation results under the controlled condition

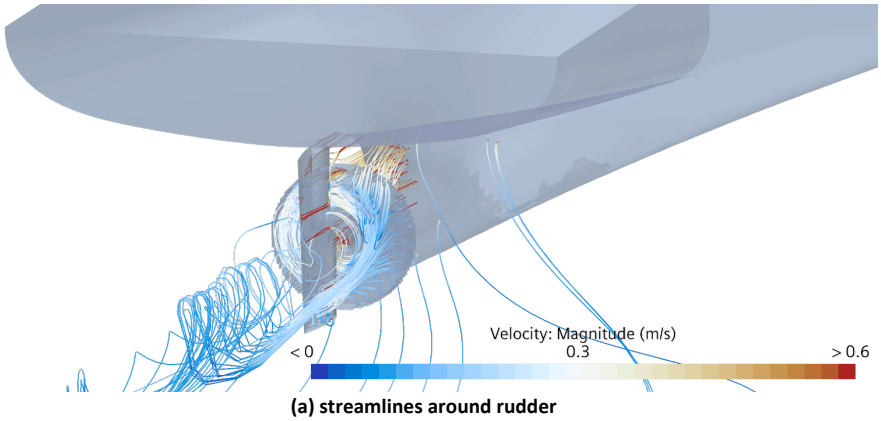

(a) streamlines around rudder

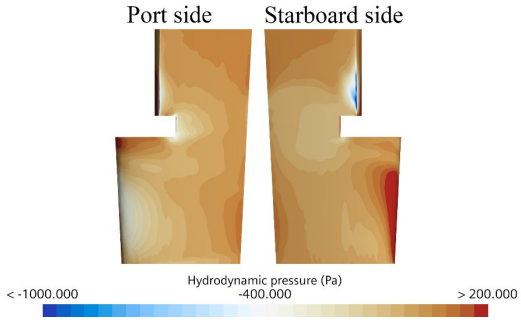

(b) pressure on rudder surface

Figure 12. Flow field results in the course-keeping process

5 CONCLUSIONS

In order to provide an in-depth analysis of the bank-effect mechanism and its influences on a moving ship in confined waterways, particularly to offer practical control guidance for ship operations in such environments, this study employs the coupled CFD method and control algorithm to investigate the course-keeping problem by direct simulations. The unsteady Reynolds Averaged Navier-Stokes (URANS) method is applied to simulate the viscous flows around the ship, and the overset mesh technique combined with the PD algorithm is adopted to realize the dynamic rudder deflection during course keeping. To address the challenges in traditional free-running simulations, this study develops a virtual bank method to simplify the modeling of bank wall effects with appropriate effectiveness. In this approach, the bank-induced forces and moments are directly imposed on the ship through formulas in terms of hydrodynamic parameters, and are added to the open-water simulations as external forces and moments.

Based on the developed method, two types of scenarios of a KCS model moving in confined waterways are investigated: one is the ship navigating with an initial off-centerline displacement, and the other is the ship navigating with an initial heading angle. Free-running simulations of the ship in a confined waterway are performed, where the rudder is controlled to maintain the zero heading angle. The predicted ship trajectories demonstrate that, the ship without the controller gradually deviates from the desired course and ultimately collides with the waterway bank in both scenarios. In contrast, the simulation results under the controlled condition show that the ship successfully achieves course-keeping in the same scenarios. However, the ship trajectory under control actions deviates approximately 0.2 m from the centerline, attributed to the selected course-keeping goal with zero heading angle only. The flow field analyses further reveal that this deviation is also caused by the asymmetrical flow field around the rudder, generated by the propeller rotation. The asymmetrical flow induces additional hydrodynamic sway forces and yaw moments, forcing the ship to deviate from the centerline slightly. This deviation allows the bank-induced forces and moments to counterbalance the additional hydrodynamic impacts, enabling the ship to maintain the target course.

In this paper, a moderate confined-water condition (h/d = 2.0 and Fr_h = 0.309) is selected to assess the feasibility of the developed method. In the future, more challenging conditions, such as smaller under-keel clearance, narrower waterways, or higher ship speeds, will be investigated to provide a more comprehensive evaluation of the robustness and applicability of the method. In addition to the course keeping without variation of heading angle by the developed method, the path following along a predetermined course to keep a distance from the bank for safe navigation in the practical application will be considered in the future study as well.

6 ACKNOWLEDGEMENTS

This work is supported by the State Key Laboratory of Maritime Technology and Safety, the National Natural Science Foundation of China (Grant No. 51979164) and the Fundamental Research Funds for the Central Universities.

7 REFERENCES

Aram, S., Mucha, P., 2023. Computational fluid dynamics analysis of different propeller models for a ship maneuvering in calm water. Ocean Eng. 276, 114226. https://doi.org/10.1016/j.oceaneng.2023.114226.

Carrica, P.M., Mofidi, A., Eloot, K., Delefortrie, G., 2016. Direct simulation and experimental study of zigzag maneuver of KCS in shallow water. Ocean Eng. 112, 117–133. https://doi.org/10.1016/j.oceaneng.2015.12.008.

Degrieck, A., Uyttersprot, B., Sutulo, S., Guedes Soares, C., Van Hoydonck, W., Vantorre, M., Lataire, E., 2021. Hydrodynamic ship-ship and ship-bank interaction: A comparative numerical study. Ocean Eng. 230, 108970. https://doi.org/10.1016/j.oceaneng.2021.108970.

Delefortrie, G., Eloot, K., Mostaert, F., 2012. SIMMAN 2014 report: Execution of Model Tests with KCS and KVLCC2. Flanders Hydraulics Research.

Delefortrie, G., Verwilligen, J., Eloot, K., Lataire, E., 2024a. Bank interaction effects on ships in 6 DOF. Ocean Eng. 310, 118614. https://doi.org/10.1016/j.oceaneng.2024.118614.

Delefortrie, G., Verwilligen, J., Kochanowski, C., Pinkster, J.A., Yuan, Z.M., Liu, Y.H., Kastens, M., Van Hoydonck, W., Pinkster, H.J.M., Lataire, E., 2024b. Unsteady ship–bank interaction: a comparison between experimental and computational predictions. Ship Technol. Res. 71 (1), 33–57. https://doi.org/10.1080/09377255.2023.2275372.

Deng, G., Queutey, P., Wackers, J., Visonneau, M., Guilmineau, E., Leroyer, A., 2022. Assessment of ship maneuvering simulation with different propeller models. J. Hydrodyn. 34 (3), 422–433. https://doi.org/10.1007/s42241-022-0039-y.

Fujino, M., 1968. Experimental studies on ship manoeuvrability in restricted waters - Part I. Int. Shipbuild. Prog. 15 (168), 279–301. https://doi.org/10.3233/ISP-1968-1516801.

Fujino, M., 1970. Experimental studies on ship manoeuvrability in restricted waters - Part II. Int. Shipbuild. Prog. 17 (186), 45–65. https://doi.org/10.3233/ISP-1968-1516801.

Kim, D., Tezdogan, T., Incecik, A., 2022. Hydrodynamic analysis of ship manoeuvrability in shallow water using high-fidelity URANS computations. Appl. Ocean Res. 123, 103176. https://doi.org/10.1016/j.apor.2022.103176.

Kim, D., Yim, J., Song, S., Park, J.B., Kim, J., Yu, Y., Elsherbiny, K., Tezdogan, T., 2023. Path-following control problem for maritime autonomous surface ships (MASS) in adverse weather conditions at low speeds. Ocean Eng. 287, 115860. https://doi.org/10.1016/j.oceaneng.2023.115860.

Lataire, E., Vantorre, M., Eloot, K., 2009. Systematic model tests on ship-bank interaction effects, in: Proceedings of the International Conference on Ship Manoeuvring in Shallow and Confined Water: Bank Effects, Antwerp, Belgium, 9–22. http://hdl.handle.net/1854/LU-663477.

Lee, S., 2023. Hydrodynamic interaction forces on different ship types under various operating conditions in restricted waters. Ocean Eng. 267, 113325. https://doi.org/10.1016/j.oceaneng.2022.113325.

Liu, H., Ma, N., Gu, X., 2021. CFD prediction of ship-bank interaction for KCS under extreme conditions. J. Mar. Sci. Technol. 26 (4), 1062–1077. https://doi.org/10.1007/s00773-021-00798-x.

Menter, F., 1993. Zonal two equation k-ω turbulence models for aerodynamic flows, in: Proceedings of the 24th Fluid Dynamics Conference. Orlando, Florida, USA. https://doi.org/10.2514/6.1993-2906.

Mucha, P., Aram, S., Radosavljevic, D., Singh, J., Wheeler, M., 2023. Propeller modeling for ship maneuvering simulations in Simcenter STAR-CCM+, in: Proceedings of the 25th Numerical Towing Tank Symposium (NuTTS). Ericeira, Portugal.

Norrbin, N.H., 1975. Manoeuvring in confined waters: interaction phenomena due to side banks or other ships, in: Proceedings of the 14th International Towing Tank Conference. Ottawa, Canada, pp. 450–486.

Ren, H., Xu, C., Zhou, X., Sutulo, S., Guedes Soares, C., 2020. A numerical method for calculation of ship–ship hydrodynamics interaction in shallow water accounting for sinkage and trim. J. Offshore Mech. Arct. Eng. 142 (5). https://doi.org/10.1115/1.4046484.

Sano, M., Yasukawa, H., Hata, H., 2012. Experimental study on ship operation in close proximity to bank channel, in: Proceedings of the International Conference on Marine Simulation and Ship Maneuverability (MARSIM 2012). Singapore.

Sano, M., Yasukawa, H., Hata, H., 2014. Directional stability of a ship in close proximity to channel wall. J. Mar. Sci. Technol. 19 (4), 376–393. https://doi.org/10.1007/s00773-014-0271-4.

Sørensen, J.N., 2022. Aerodynamic Analysis of Wind Turbines, in: Comprehensive Renewable Energy (Second Edition). pp. 172–193. https://doi.org/10.1016/B978-0-12-819727-1.00127-8.

Terziev, M., Liu, Y., Yuan, Z., Incecik, A., 2024. The resistance of a trans-critically accelerating ship in shallow water. Ship Technol. Res. 71 (1), 14–32. https://doi.org/10.1080/09377255.2023.2252232.

Van Hoydonck, W., Toxopeus, S., Eloot, K., Bhawsinka, K., Queutey, P., Visonneau, M., 2019. Bank effects for KVLCC2. J. Mar. Sci. Technol. 24 (1), 174–199. https://doi.org/10.1007/s00773-018-0545-3.

Van Zwijnsvoorde, T., Delefortrie, G., Lataire, E., 2022. Passing ship effects in shallow and confined water: open model test data for validation purposes, in: Proceedings of the 6th MASHCON International Conference on Ship Manoeuvring in Shallow and Confined Water. Glasgow, UK, pp. 255–283. http://hdl.handle.net/1854/LU-01H0HW8J5FDQDVEMB3PGZ2ZSX2.

Vantorre, M., Delefortrie, G., Eloot, K., Laforce, E., 2003. Experimental investigation of ship-bank interaction forces, in: Proceedings of the International Conference on Marine Simulation and Ship Maneuverability. Kanazawa, Japan, pp. RC-31-31–RC-31-39. http://hdl.handle.net/1854/LU-298476.

Vantorre, M., Verzhbitskaya, E., Laforce, E., 2002. Model test based formulations of ship-ship interaction forces. Ship Technol. Res. 49, 124–141. http://hdl.handle.net/1854/LU-160369.

Wang, J., Zou, L., Wan, D., 2017. CFD simulations of free running ship under course keeping control. Ocean Eng. 141, 450–464. https://doi.org/10.1016/j.oceaneng.2017.06.052.

Xu, C., Zhou, X., Ren, H., Sutulo, S., Guedes Soares, C., 2024. Real-time calculation of ship to ship hydrodynamic interaction in shallow waters with adaptive mesh refinement. Ocean Eng. 295, 116943. https://doi.org/10.1016/j.oceaneng.2024.116943.

Yao, J.X., Zou, Z.J., 2010. Calculation of ship squat in restricted waterways by using a 3D panel method. J. Hydrodyn. 22 (5, Supplement 1), 489–494. https://doi.org/10.1016/S1001-6058(09)60241-9.

Yasukawa, H., 2019. Maneuvering hydrodynamic derivatives and course stability of a ship close to a bank. Ocean Eng. 188, 106149. https://doi.org/10.1016/j.oceaneng.2019.106149.

Yuan, Z.M., Incecik, A., 2016. Investigation of ship-bank, ship-bottom and ship-ship interactions by using potential flow method, in: Proceedings of the 4th International Conference on Ship Manoeuvring in Shallow and Confined Water. Hamburg, Germany, pp. 83–92.

Yuan, Z.M., 2019. Ship hydrodynamics in confined waterways. J. Ship Res. 63 (01), 16–29. https://doi.org/10.5957/JOSR.04170020.

Zheng, Z.Q., Zou, L., Zou, Z.J., 2023. A numerical study of passing ship effects on a moored ship in confined waterways with new benchmark cases. Ocean Eng. 280, 114643. https://doi.org/10.1016/j.oceaneng.2023.114643.

Zhou, X., Sutulo, S., Guedes Soares, C., 2012. Computation of ship hydrodynamic interaction forces in restricted waters using potential theory. J. Mar. Sci. Appl. 11 (3), 265–275. https://doi.org/10.1007/s11804-012-1132-3.

Zou, L., 2012. CFD Predictions Including Verification and Validation of Hydrodynamic Forces and Moments on a Ship in Restricted Waters. Chalmers University of Technology, Gothenburg, Sweden.

Zou, L., Larsson, L., 2013. Computational fluid dynamics (CFD) prediction of bank effects including verification and validation. J. Mar. Sci. Technol. 18 (3), 310–323. https://doi.org/10.1007/s00773-012-0209-7.

8 AUTHORS BIOGRAPHY

Zi-Qiang Zheng is a PhD student at School of Ocean and Civil Engineering, Shanghai Jiao Tong University. He majors in ship hydrodynamic performances in restricted waters based on numerical methods, etc.

Yu He is a PhD student at School of Ocean and Civil Engineering, Shanghai Jiao Tong University. He majors in ship motion control, etc.

Lu Zou holds the current position of Associate Professor at School of Ocean and Civil Engineering, Shanghai Jiao Tong University. Her major research interest is ship hydrodynamic problems in confined waters, modeling of ship maneuvering motion, ship motion control, etc.

Zao-Jian Zou is a retired professor at School of Ocean and Civil Engineering, Shanghai Jiao Tong University. His previous experience includes PI of projects on maneuvering and control of ships and other marine vehicles. He was a member of the 22nd, 23rd, 25th and 26th ITTC Maneuvering Committee.